

Measure an array of cytokines in COVID-19 samples
with our multiplex flow cytometry assays.

Read our app note ►



Domain-Specific and Stage-Intrinsic Changes in *Tcrb* Conformation during Thymocyte Development

This information is current as
of February 26, 2022.

Kinjal Majumder, Levi J. Rupp, Katherine S. Yang-Iott,
Olivia I. Koues, Katherine E. Kyle, Craig H. Bassing and
Eugene M. Oltz

J Immunol 2015; 195:1262-1272; Prepublished online 22
June 2015;
doi: 10.4049/jimmunol.1500692
<http://www.jimmunol.org/content/195/3/1262>

**Supplementary
Material** <http://www.jimmunol.org/content/suppl/2015/06/20/jimmunol.1500692.DCSupplemental>

References This article **cites 52 articles**, 20 of which you can access for free at:
<http://www.jimmunol.org/content/195/3/1262.full#ref-list-1>

Why *The JI*? [Submit online.](#)

- **Rapid Reviews! 30 days*** from submission to initial decision
- **No Triage!** Every submission reviewed by practicing scientists
- **Fast Publication!** 4 weeks from acceptance to publication

**average*

Subscription Information about subscribing to *The Journal of Immunology* is online at:
<http://jimmunol.org/subscription>

Permissions Submit copyright permission requests at:
<http://www.aai.org/About/Publications/JI/copyright.html>

Email Alerts Receive free email-alerts when new articles cite this article. Sign up at:
<http://jimmunol.org/alerts>



Domain-Specific and Stage-Intrinsic Changes in *Tcrb* Conformation during Thymocyte Development

Kinjal Majumder,^{*,1} Levi J. Rupp,^{†,‡,1} Katherine S. Yang-Iott,^{†,‡} Olivia I. Koues,^{*} Katherine E. Kyle,^{*} Craig H. Bassing,^{†,‡} and Eugene M. Oltz^{*}

Considerable cross-talk exists between mechanisms controlling genome architecture and gene expression. AgR loci are excellent models for these processes because they are regulated at both conformational and transcriptional levels to facilitate their assembly by V(D)J recombination. Upon commitment to the double-negative stage of T cell development, *Tcrb* adopts a compact conformation that promotes long-range recombination between V β gene segments (*Trbvs*) and their D β J β targets. Formation of a functional V β D β J β join signals for robust proliferation of double-negative thymocytes and their differentiation into double-positive (DP) cells, where *Trbv* recombination is squelched (allelic exclusion). DP differentiation also is accompanied by decontraction of *Tcrb*, which has been thought to separate the entire *Trbv* cluster from D β J β segments (spatial segregation-based model for allelic exclusion). However, DP cells also repress transcription of unrearranged *Trbvs*, which may contribute to allelic exclusion. We performed a more detailed study of developmental changes in *Tcrb* topology and found that only the most distal portion of the *Trbv* cluster separates from D β J β segments in DP thymocytes, leaving most *Trbvs* spatially available for rearrangement. Preferential dissociation of distal *Trbvs* is independent of robust proliferation or changes in transcription, chromatin, or architectural factors, which are coordinately regulated across the entire *Trbv* cluster. Segregation of distal *Trbvs* also occurs on alleles harboring a functional V β D β J β join, suggesting that this process is independent of rearrangement status and is DP intrinsic. Our finding that most *Trbvs* remain associated with D β J β targets in DP cells revises allelic exclusion models from their current conformation-dominant to a transcription-dominant formulation. *The Journal of Immunology*, 2015, 195: 1262–1272.

The assembly and expression of AgR genes is controlled at multiple levels, including chromatin accessibility, transcription, and changes in three-dimensional (3D) conformation (1–4). Because AgR genes span large regions of mammalian genomes, which are independently activated and repressed during lymphocyte development, these loci serve as excellent models to study long-range mechanisms that coordinate gene expression (5). In addition to gene expression, regulatory mechanisms shared among AgR loci orchestrate the process of V(D)J recombination (4), which assembles exons encoding their variable regions from large arrays of V, D, and J gene segments. The availability of gene segments for recombination within each AgR locus is modulated during lymphocyte development to guide their ordered and tissue-specific assembly, as well as to enforce allelic exclusion, a process that ensures the production of only

a single, functional allele for each AgR gene in most B and T cells (6). Proper regulation of V(D)J recombination is essential for generating a diverse repertoire of AgRs, driving lymphocyte development, and avoiding chromosomal translocations that characterize many forms of leukemia and lymphoma (7–9).

All AgR loci have at least one powerful enhancer element that activates promoters associated with the most proximal clusters of gene segments, revising the chromatin landscape to facilitate the deposition of the histone modification H3K4me3, an epigenetic mark recognized by RAG2 (10–12), which, together with RAG1, are lymphocyte-specific components of the V(D)J recombinase. Because the enhancer-proximal gene segments are decorated with such a high density of RAG proteins, these regions have been coined recombination centers (RCs) (13). As an example, the *Tcrb* enhancer, called E β , is activated upon commitment of multipotent progenitors to the

^{*}Department of Pathology and Immunology, Washington University School of Medicine, St. Louis, MO 63110; [†]Division of Cancer Pathobiology, Department of Pathology and Laboratory Medicine, Center for Childhood Cancer Research, Children's Hospital of Philadelphia, Philadelphia, PA 19104; and [‡]Abramson Family Cancer Research Institute, Cell and Molecular Biology Graduate Program, Department of Pathology and Laboratory Medicine, Perelman School of Medicine at the University of Pennsylvania, Philadelphia, PA 19104

¹K.M. and L.J.R. contributed equally to this work.

Received for publication March 24, 2015. Accepted for publication May 31, 2015.

This work was supported by National Institutes of Health Grants AI 079732 and AI 118852 (to E.M.O.), AI 112621 (to C.H.B.), and CA090547 (to O.I.K.), as well as by a Leukemia and Lymphoma Society Scholar Award (to C.H.B.). We thank the Genome Technology Access Center in the Department of Genetics at Washington University School of Medicine for help with genomic analysis. This center is partially supported by National Cancer Institute Cancer Center Support Grant P30 CA91842 to the Siteman Cancer Center, by Institute of Clinical and Translational Sciences Clinical and Translational Science Award Grant UL1 TR000448 from the National Center for Research Resources, a component of the National Institutes of Health, and by the National Institutes of Health Roadmap for Medical Research.

This publication is solely the responsibility of the authors and does not necessarily represent the official view of the National Center for Research Resources or the National Institutes of Health.

The 4C-seq data presented in this article have been submitted to the Gene Expression Omnibus repository (<http://www.ncbi.nlm.nih.gov/genbank>) under accession number GSE68955.

Address correspondence and reprint requests to Dr. Eugene M. Oltz or Dr. Craig H. Bassing, Department of Pathology and Immunology, Washington University School of Medicine, 660 Euclid Avenue Box 8118, 7728 CSRB, St. Louis, MO 63110 (E.M.O.) or Children's Hospital of Philadelphia, 4054 Colket Translational Research Building, 3501 Civic Center Boulevard, Philadelphia, PA 19104 (C.H.B.). E-mail addresses: eoltz@wustl.edu (E.M.O.) or bassing@mail.med.upenn.edu (C.H.B.)

The online version of this article contains supplemental material.

Abbreviations used in this article: BE, boundary element; 3C, chromosome conformation capture; 4C, circular chromosome conformation capture; ChIP, chromatin immunoprecipitation; CTCF, CCCTC binding factor; 3D, three-dimensional; DN, double-negative; DP, double-positive; E β , *Tcrb* enhancer; FISH, fluorescence in situ hybridization; 5'PC, 5' *Prss2* CCCTC binding factor site; qPCR, quantitative PCR; RC, recombination center; -seq, coupled with high-throughput sequencing.

Copyright © 2015 by The American Association of Immunologists, Inc. 0022-1767/15/\$25.00

T cell lineage in the thymus (14, 15). In turn, E β associates with promoters located in each of the proximal D β J β clusters, triggering 1) robust transcription, 2) chromatin accessibility at the unrearranged gene segments, 3) RAG-1/2 deposition, and 4) D β -to-J β recombination, which occurs over short distances (16).

Complete assembly of V region exons for *Tcrb*, *Tcrd*, and *Igh* requires a second round of recombination between joined DJ elements in the RC and one of many V segments splayed out over large genomic distances. Numerous studies have shown that the second, long-range V-to-DJ recombination event is facilitated by conformational changes at these loci (17–19). As an example, upon commitment to the double-negative (DN) stage of T cell development, the most distal ends of *Tcrb*, which are separated by >500 kb in the linear genome, come together in 3D space, a process coined locus contraction (20, 21). *Tcrb* contraction coincides with the folding of its V β cluster into two spatially distinct domains, spanning proximal and distal portions of the *Trbv* array (22). Each of the more compact *Trbv* domains also folds into the RC, presumably via the process of locus contraction, endowing the V β segments with spatial access to D β J β substrates (7, 22). Indeed, we have shown that *Trbv* usage is largely limited by the activities of their associated promoters rather than by their absolute proximity to the RC (7), suggesting that all V β gene segments have crossed a spatial threshold required for RAG-mediated recombination.

Interactions between the distal *Trbv* domain and the RC appear focused on a site called 5'PC, which binds the architectural protein CCTC binding factor (CTCF) and is located ~25 kb upstream of the D β J β cluster (22). Genome-wide studies have revealed that when CTCF is bound to pairs of sites with convergent orientations, CTCF–CTCF dimerization can generate structural loops (23, 24). In many cases, such chromosomal loops are stabilized via association of CTCF dimers with cohesin, a ring-like complex that locks the loop bases into place (25). Of note, the numerous CTCF sites scattered throughout both *Trbv* domains are all in the same orientation, which favors their association with the 5'PC site near the RC. A similar mechanism of long-range tethering appears to be at play for other AgR loci, with V segments forming distinct domains that harbor multiple CTCF sites in a convergent orientation relative to those near the RC (26, 27). In what may be a related finding, ablation of CTCF or its key binding sites in AgR loci disrupts spatial interactions and long-range V(D)J recombination (26–30).

Although locus contraction promotes long-range recombination at nearly all AgR loci, this process is developmentally dynamic. For example, when DN thymocytes generate a productive *Tcrb* allele, pre-TCR signaling induces at least 10 rounds of rapid cell division (31). These proliferating cells ultimately differentiate into the resting CD4⁺CD8⁺ (double-positive [DP]) subset, in which distal ends of *Tcrb* separate spatially, presumably reverting to their original “decontracted” state found in multipotent progenitors (20, 21). Spatial segregation of the *Trbv* cluster from the RC is thought to help enforce allelic exclusion (20, 21), disfavoring further long-range *Tcrb* recombination, which could generate two functional AgR chains. Similar changes in contraction status have been observed at some (32, 33), but not all (34), AgR loci during developmental transitions between precursor lymphocyte subsets.

Despite these advances, developmental changes in conformation have not been characterized for any AgR locus at a sufficient resolution to understand the precise nature of locus decontraction and its implications for allelic exclusion. We now use chromosome conformation capture technologies to probe architectural remodeling of *Tcrb* conformations during transition from the DN (contracted, V-to-DJ recombination active) to the DP stage of

thymocyte development (decontracted, V-to-DJ recombination excluded). Remarkably, we show that decontracted *Tcrb* loci in DP thymocytes retain a close association between the RC and most of the *Trbv* cluster, with only the distal portion of the V β array dissociating from this interactome. Therefore, transcriptional repression of *Trbvs*, rather than their spatial separation from the RC, may be the dominant mechanism ensuring allelic exclusion of most V β segments in DP thymocytes. Dissociation of the distal *Trbv* domain, as well as locus decontraction, is independent of gross changes in CTCF/cohesin deposition and the massive proliferative burst that accompanies DN cell differentiation to the DP stage. Importantly, we find that, in DP thymocytes, dissociation of distal *Trbv* segments also occurs on alleles harboring a functional V β D β J β rearrangement, which delete regions within *Tcrb* implicated as architectural determinants. Taken together, these findings indicate that developmental changes in *Tcrb* conformation are V β domain specific and are governed by DP-intrinsic mechanisms.

Materials and Methods

Mice

Thymocytes were harvested from Rag1^{−/−}/C57BL/6 mice directly (DN) after injection of anti-CD3 ϵ (DP) (35), or those expressing a *Tcrb* transgene (DP) (36, 37). For certain experiments (indicated in *Results*), thymocytes were isolated from mice of the following genotypes, all of which were on a mixed 129SvEv/C57BL/6 background: RAG1^{−/−}:*Tcrb*:*Ccnd3*^{−/−} (DN and DP), V β 1^{NT/NT}:Rag1^{−/−} (DP) (38), or V β 1^{NT/NT}:Lat^{−/−}:Rag1^{−/−} (DN) (39). All experiments were conducted on mice that were between 4 and 6 wk of age. Animal procedures and experimental protocols were approved by the Institutional Animal Care and Use Committees at Washington University School of Medicine in St. Louis and Children's Hospital of Philadelphia.

Chromosome conformation capture assays

Chromosome conformation capture (3C) assays were performed precisely as described (22) using 10⁷ thymocytes or pro-B cells from Rag1^{−/−} mice or from cultured 3T3 fibroblasts. Cross-linking efficiencies were measured using TaqMan–quantitative PCR (qPCR) assays with primers and probes shown in Supplemental Table I.

Circular chromosome conformation capture coupled with high-throughput sequencing

Circular chromosome conformation capture (4C) assays were performed with HindIII as the primary restriction enzyme for cutting cross-linked chromatin. The HindIII-digested DNA was ligated using the 3C protocol and resuspended in buffer EB (100 μ l, Qiagen). Secondary enzyme digestion was performed with NlaIII (100 U, overnight). After heat inactivation, the digested DNA was religated to generate circularized products of interaction partners, purified by phenol/chloroform extraction, precipitated in isopropanol, resuspended in buffer EB (100 μ l), and quantified as described previously (40). Inverse PCR was performed on the circularized DNA using primers within HindIII–NlaIII fragments at E β or at *Trbv5* (see Supplemental Table I). Inverse PCR products were diluted 1:100 in TE buffer and used as templates for nested inverse PCRs (see Supplemental Table I), yielding the 4C DNA libraries.

Purified 4C DNA (100 ng, PCR purification kit, Qiagen) was used for indexed library preparation. On average, eight indexed libraries were pooled and subjected to 42-bp single-end sequencing according to the manufacturer's protocol (HiSeq2000 from Illumina, San Diego, CA). Sequence tags were aligned to the reference genome (build MM9) with Bowtie (41). The r3C-seq package (42) was used to calculate reads per million for each sample and identify anchor interaction regions. EMBOSS (43) was used to generate a genome-wide map of the HindIII restriction fragments for assignment of reads. To compare between samples, reads per million values for each fragment were quantile normalized. For visualization of the 4C coupled with high-throughput sequencing (4C-seq) data, a running mean was calculated using a window size of three contiguous HindIII fragments (40).

Public data sources

Chromatin immunoprecipitation (ChIP)–seq data were obtained from the Gene Expression Omnibus repository for CTCF (accession number GSE41739, see ref. 36), as well as H3K4me1 and H3K4me3 (accession number GSE55635, see ref. 44) (<http://www.ncbi.nlm.nih.gov/genbank>).

3D fluorescence in situ hybridization

3D fluorescence in situ hybridization (3D-FISH) assays were performed with *Tcrb* bacterial artificial chromosome probes spanning *Trbv1* (RP23-75P5) and trypsinogen (RP23-203H5) precisely as described (22). Imaged data were analyzed using ImageJ as described (22).

ChIP assays

ChIP assays were performed as described previously (22) using the following Abs: CTCF (Rockland Immunochemicals, 600-401-C42), RAD21 (Abcam, ab992), H3Ac (EMD Millipore, 06-599), H3K4me2 (Abcam, ab32356), and IgG (Santa Cruz Biotechnology, sc-2027). ChIP assays were analyzed by qPCR with primer combinations shown in Supplemental Table 1.

RNA extraction and germline transcription

RNA was prepared from 0.5 to 1 million cells using TRIzol (Invitrogen). cDNA was generated from 1 μ g RNA using murine leukemia virus reverse transcriptase (New England Biolabs) and analyzed by qPCR with primer combinations provided in Supplemental Table 1.

Results

Only distal *Trbv* segments dissociate from the RC in DP thymocytes

Repression of *Tcrb* gene assembly in DP cells correlates with significantly attenuated expression of unrearranged *Trbv* segments (45, 46) and spatial segregation of the extreme 5' and 3' ends of the locus, that is, decontraction (20–22). The latter cell imaging data have been extrapolated into models suggesting that *Tcrb* reverts to an extended conformation in DP thymocytes, with a loss of all RC–*Trbv* interactions (10, 20). To study developmental changes in *Tcrb* conformation at a higher resolution, we performed 4C-seq, an approach that allows us to measure the cross-linking efficiency of a given restriction fragment (viewpoint) with the entire genome (accession number GSE68955). The 4C-seq assays were performed with cross-linked chromatin from RAG-deficient DN thymocytes or RAG-deficient animals injected with anti-CD3 ϵ Ab, which drives differentiation into the DP stage (35). Both DN and DP thymocytes from these mice retain *Tcrb* gene segments in their germline configuration due to a lack of recombinase activity (35). As shown in Fig. 1A, the *Tcrb* enhancer region (E β) associates with the entire *Trbv* cluster in DN thymocytes, which is consistent with prior findings (7, 20, 22). Surprisingly, many of these long-range interactions are maintained in DP thymocytes, despite *Tcrb* decontraction, as ascertained by 3D-FISH using probes for the 5' and 3' ends of the locus (Fig. 1B). Notably, only the distal region of the *Trbv* cluster appears to dissociate uniformly from this RC viewpoint upon transition to the DP stage, suggesting that decontraction does not involve the entire *Tcrb* locus in DP thymocytes.

To further validate the compartmentalized changes in *Tcrb* conformation during thymocyte development, we performed 3C-qPCR to focus on specific interactions between pairs of restriction fragments. We find that E β association with *Trbv* segments spread over the proximal half of the cluster is unperturbed when comparing DN to DP thymocytes generated by anti-CD3 ϵ injection (Fig. 1C). In contrast, E β association with the more distal *Trbv* segments diminishes significantly in these DP cells (Fig. 1C). The changes in long-range *Trbv*–RC interactions, as well as reversal of locus contraction, are recapitulated in RAG-deficient DP thymocytes when their development is driven by the expression of a *Tcrb* transgene (Fig. 1B, 1D) (36, 37). The latter data preclude the possibility that superphysiologic signaling by anti-CD3 ϵ is responsible for our observations.

3C analyses using complementary viewpoints in the *Trbv* cluster further confirmed our findings from 4C-seq. For example, robust

cross-linking between the distal *Trbv5* region and two restriction fragments in the D β J β cluster is observed in DN thymocytes, but it is reduced to near background levels in DP cells (Fig. 1E, left). As expected, *Trbv5* association with 5'PC, the CTCF binding element that serves as a tether for long-range interactions between the RC and distal V β region (22), is also lost in DP thymocytes (Fig. 1E, left). In sharp contrast, associations between the more proximal *Trbv23* and the 5'PC-RC portion of the locus are unaffected by the DN to DP transition (Fig. 1E, right), even though these regions are separated by >200 kb in the linear genome. Preferential dissociation of the distal *Trbv* region from the RC does not correlate with domain-specific changes in transcription, which is reduced in DP thymocytes for V β segments within both the proximal and distal domains, regardless of the stimulus employed to generate DP cells (Fig. 1F). As expected, transitioning to the DP stage has no effect on or augments transcription of the RC and the proximal *Trbv31* gene segment, which is located adjacent to the RC (39, 47). Similar to transcription, histone modifications associated with active promoters (H3K4me3), or simply open chromatin (H3K4me1) (44), are coordinately regulated within the entire *Trbv* cluster when comparing ChIP-seq data from DN and DP thymocytes (Fig. 1G). We conclude that dissociation of V β segments from the RC is highly restricted to the distal region of the *Trbv* cluster and is independent of changes in transcription and chromatin, which occur over the entire *Trbv* cluster.

Trbv domains remain folded in DP thymocytes

In DN thymocytes, distal and proximal regions of the *Trbv* cluster fold into separate spatial domains that associate with the RC in 5'PC-dependent and -independent manners, respectively (22). Additional 4C experiments using the distal *Trbv5* region as a viewpoint revealed that its association with other distal V β segments is retained in DP thymocytes (Fig. 2A). However, *Trbv5* becomes spatially segregated from *Trbv* segments in the RC-proximal portion of the cluster during this developmental transition (Fig. 2A).

3C data using distal and proximal *Trbv* viewpoints confirmed that each domain retains its internal, folded conformation, but only the distal V β domain strays from the RC in DP thymocytes (Figs. 1E, 2B). For example, association between *Trbv5* and *Trbv1* within the distal domain is unchanged in DN versus DP cells, whereas interaction between *Trbv5* (distal) and *Trbv12-2* (proximal) diminishes significantly (Fig. 2B, left), despite a nearly equal linear distance between *Trbv5* and each of these two gene segments. Conversely, *Trbv23*, which is in the proximal domain, cross-links with equal efficiencies to the proximal *Trbv12-2* segment in DN and DP cells, but with a reduced efficiency to the distal *Trbv1* segment in DP thymocytes (Fig. 2B, right).

These conformational data indicate that the developmental transition of DN to DP thymocytes disrupts long-range interactions between the RC and the distal V β domain, which remains in a folded conformation. In contrast, RC interactions with the folded cluster of proximal *Trbv* segments are fully retained upon differentiation to the DP stage. Thus, we conclude that repression of recombination at proximal *Trbv* segments in DP cells is independent of spatial dissociation from their target substrates in the D β J β cluster.

Binding of architectural proteins and chromatin boundaries are largely unaltered in DN and DP thymocytes

The architectural protein CTCF facilitates the formation of structural loops in metazoan genomes, including those found in AgR loci (23, 24). Many loops are stabilized via the association of

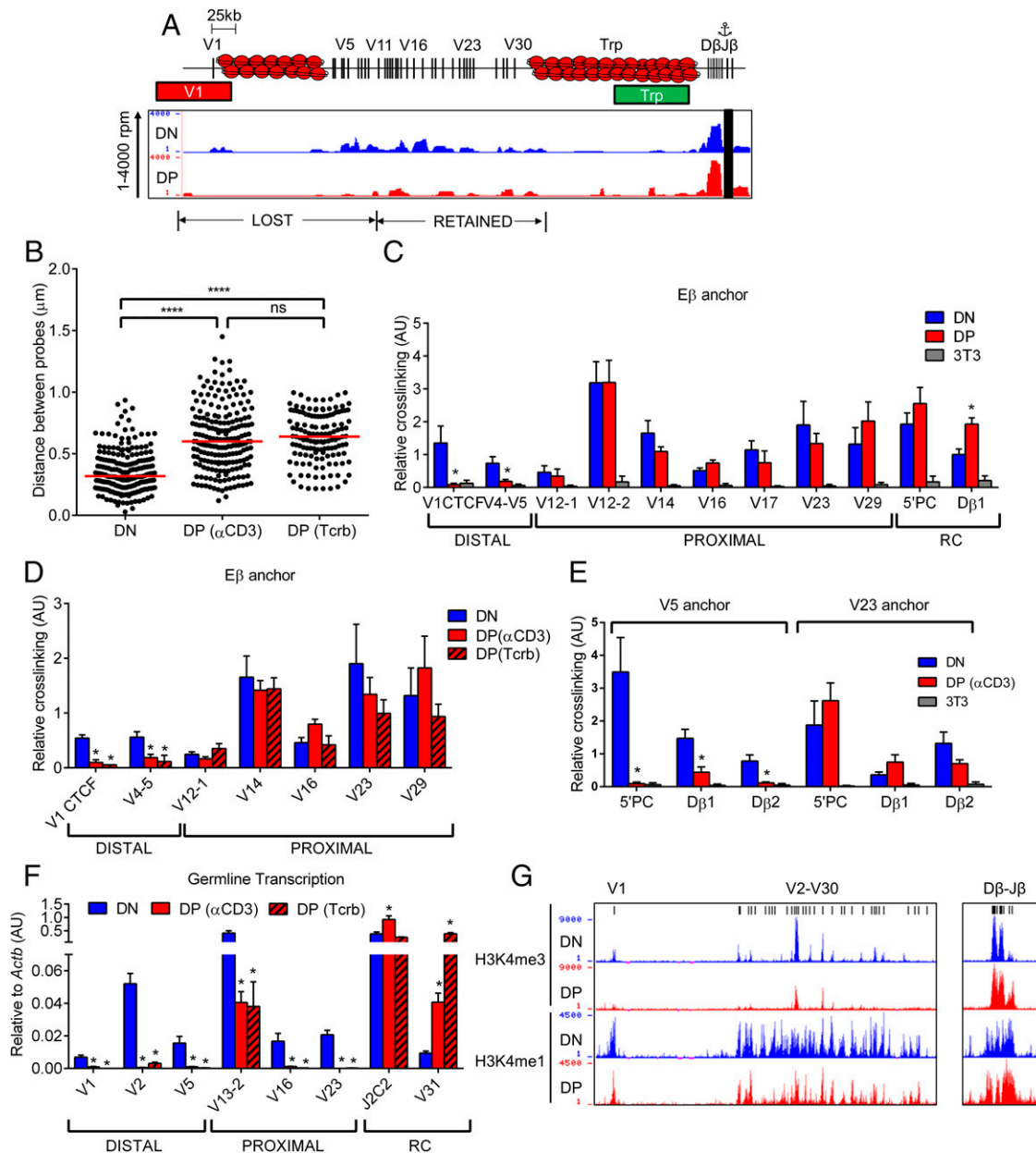


FIGURE 1. Specific dissociation of distal *Trbv* segments in DP thymocytes. **(A) Top**, Schematic of mouse *Tcrb* showing inactive trypsinogen regions as red nucleosomes. **Bottom**, Long-range interaction of Eβ viewpoint in *RAG1*^{-/-} DN thymocytes (blue) compared with *RAG1*^{-/-} DP thymocytes (red), which were generated by anti-CD3ε injections. These data represent an average of three independent experiments with values reflecting running means of three adjacent fragments as described (40). Location of the Eβ viewpoint is denoted by a black bar, as well as an anchor symbol above the cartoon. The y-axis represents normalized reads per million (rpm, see *Materials and Methods* for details) with a scale of 1 to 4000. **(B)** 3D-FISH assays for *Tcrb* contraction using probes spanning the *Trbv1* and trypsinogen gene cluster [shown as red and green bars, respectively, in (A)]. Data are presented for thymocytes from *RAG1*^{-/-} animals (DN) or *RAG1*^{-/-} mice treated with anti-CD3ε or expressing a *Tcrb* transgene (DP). Results are presented as scatter plots of distances between probe foci and represent three independent preparations of slides. Significant differences in the 3D-FISH assays are denoted as *****p* < 0.00001 (one-way ANOVA, Tukey post hoc test), and ns represents nonsignificant differences in median distances. **(C)** 3C analysis was performed with the Eβ viewpoint in DN and DP thymocytes (anti-CD3ε). NIH-3T3 cells (gray) serve as controls for background levels of cross-linking to the indicated upstream *Trbv* gene segments. For all 3C panels, data are presented as average of three independent experiments ± SEM and relative cross-linking values were calculated as described (22). Significant differences between DN and DP thymocytes in all 3C-qPCR assays are denoted as **p* < 0.05 (Student *t* test). **(D)** 3C analysis using the Eβ viewpoint to compare DP thymocytes from *RAG1*^{-/-} mice generated with either anti-CD3ε treatment (solid red) or expression of a *Tcrb* transgene (red with black diagonals). **(E)** 3C analysis was performed in DN, DP, and 3T3 cells using a *Trbv5* (distal domain) or a *Trbv23* viewpoint (proximal domain). **(F)** Germline transcription of the indicated regions was quantified relative to mRNA levels for *Actb* in DN and DP thymocytes (generated in *RAG*-deficient mice by anti-CD3ε injections or by expression of a *Tcrb* transgene) as described previously (22). All qPCR values are presented as means ± SEM of at least three independent experiments. Significant differences between DN and DP thymocytes are denoted as **p* < 0.05 (Student *t* test). **(G)** Genome browser tracks of ChIP-seq data showing levels of H3K4me3 and H3K4me1 on *Tcrb* in DN (blue) and DP (red) thymocytes. ChIP-seq data were obtained from a published study (44).

CTCF with the ring-like cohesin complex, which is thought to ensnare the bases of chromatin loops (25). To determine whether the loss of distal *Trbv*–RC contacts in DP thymocytes is mecha-

nistically related to reduced binding of supporting architectural complexes, we performed ChIP-qPCR assays using chromatin from DN (*RAG1*^{-/-}) and DP subsets (*RAG1*^{-/-}:anti-CD3ε).

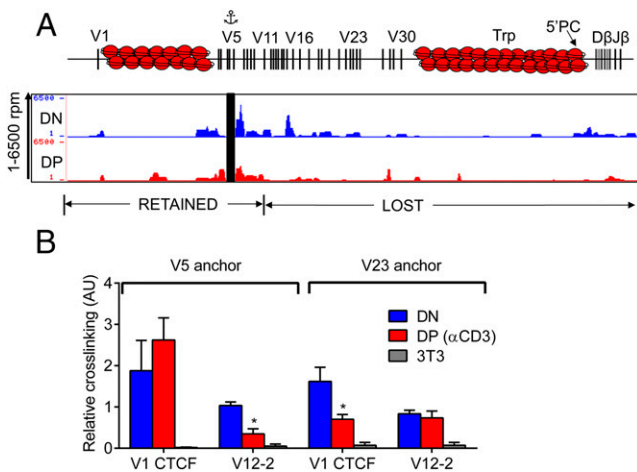


FIGURE 2. Interactions within each *Trbv* domain are unchanged in DN and DP thymocytes. **(A)** Top, Schematic of *Tcrb*, as described for Fig. 1A. Bottom, Long-range interactions using a *Trbv5* viewpoint (anchor symbol in *Tcrb* schematic). The data are presented as an average of three independent experiments, with y-axes (reads per million [rpm]) ranging from 1 to 6500. **(B)** 3C analysis was performed with *Trbv5* and *Trbv23* viewpoints in DN and DP thymocytes, using 3T3 fibroblasts as negative controls. Significant differences between DN and DP samples are denoted as * $p < 0.05$ (Student t test).

CTCF binding sites in *Tcrb* are shown in Fig. 3A (top) as established by ChIP-seq data from RAG-deficient DN thymocytes (36). Remarkably, levels of CTCF and the cohesin subunit RAD21 are not altered significantly in DN and DP thymocytes at the vast majority of tested sites, including those in distal and proximal *Trbv* domains, as well as RC flanking sites (Fig. 3A, middle and bottom). The one exception is a modest loss of CTCF at the 5'PC site, which functions as a tether for the distal *Trbv* domain in DN cells. However, levels of RAD21 at this tethering site remain unchanged in DP when compared with DN thymocytes.

We have recently shown that the tethering function of 5'PC can be compromised, despite retention of CTCF and RAD21 binding, by deletion of a chromatin boundary element (BE) located upstream of the RC (Δ PDβ1, Fig. 3C, top) (22). Removal of the natural BE permits a spread of highly active chromatin from the RC to 5'PC, which becomes a new boundary and, in some manner, acquisition of this function compromises its ability to serve as a long-range tether (22). Thus, one potential mechanism for specific dissociation of distal *Trbv* segments would be inactivation of the RC-proximal chromatin boundary in DP thymocytes, which would in turn disarm the 5'PC tether.

Initially, we tested this possibility by monitoring RNA expression from the normally silent trypsinogen gene *Prss2*, which is activated in DN thymocytes upon deletion of the RC-proximal BE (Fig. 3B). However, *Prss2* remains transcriptionally silent in DP thymocytes, suggesting that RC-proximal boundary function remains intact in these cells. This conclusion is bolstered by ChIP assays that monitored the spread of active chromatin upstream of the RC. The invasion of active chromatin is significant in DN cells lacking the native BE (Δ PDβ1), but not in DP thymocytes (Fig. 3C). Thus, dissociation of distal *Trbv* segments in DP thymocytes is not simply due to a loss of CTCF-cohesin within this structural domain, nor is it due to a disruption of chromatin boundary function upstream of the RC, which would impair distal *Trbv* tethering to 5'PC.

Stage-specific changes in *Tcrb* conformation are independent of the DN to DP proliferative burst

Prior studies have shown that most structural loops within the genome are disrupted during mitosis and reform in resting daughter

cells (48). Developmental progression of DN thymocytes to the DP stage is associated with a robust proliferative burst. Indeed, a TCRβ⁺ DN thymocyte, on average, undergoes 10–11 rounds of division before coming to rest at the DP stage (31). Accordingly, we hypothesized that changes in *Tcrb* conformation during the DN to DP transition may require this robust proliferation, which would dissolve the DN architecture and allow its reconfiguration into the DP conformation.

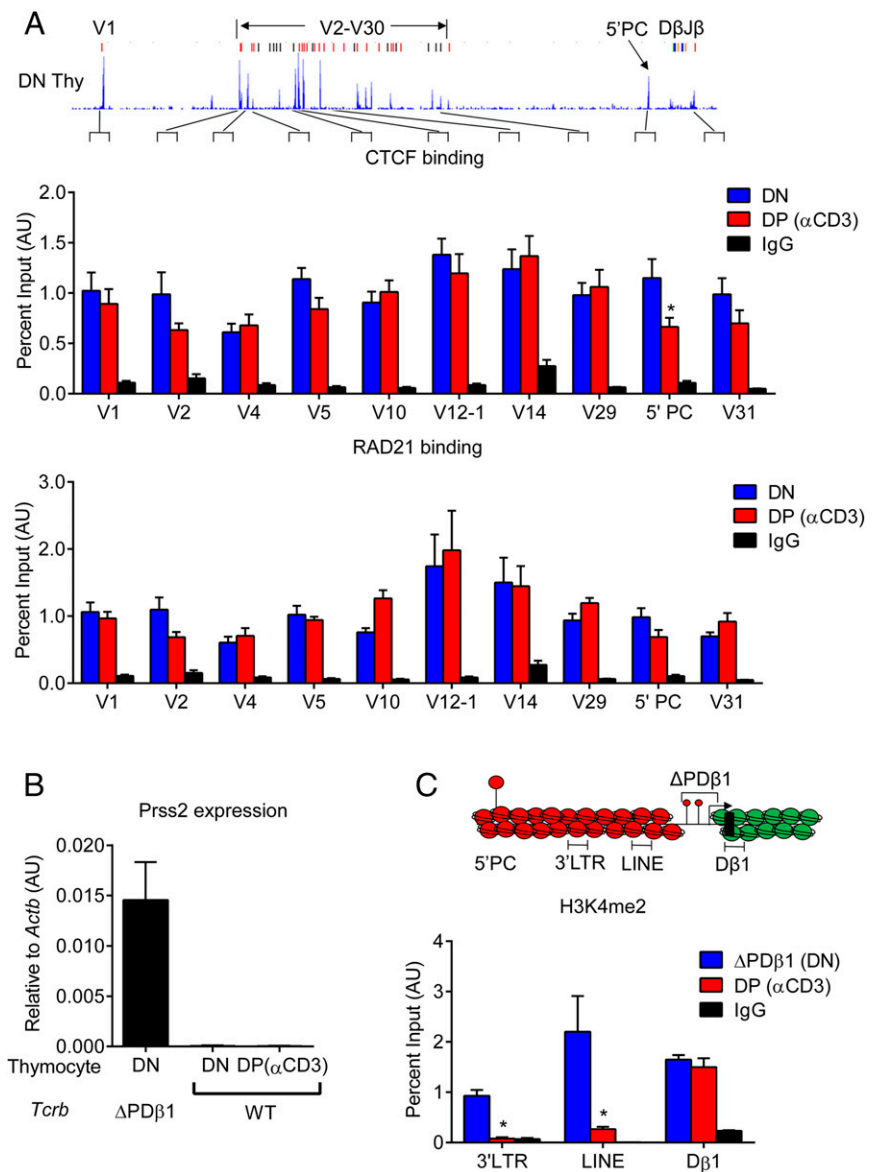
To test this hypothesis, we used mice that lacked the gene encoding a CDK4/6 regulatory subunit, cyclin D3 (*Ccnd3*^{-/-}), a defect that severely compromises thymocyte proliferation (31). When RAG1^{-/-}:*Tcrb* transgenic mice are crossed into the *Ccnd3*-deficient background (RAG1^{-/-}:*Ccnd3*^{-/-}:*Tcrb*), thymocytes progress to the DP stage of development without the normal proliferative burst (31). These cellular defects are highlighted in Fig. 4A. Compared with RAG1^{-/-}:*Tcrb* mice, in which the TCRβ-driven proliferative burst generates large numbers of DP thymocytes (1.2×10^8) (31, 36), RAG1^{-/-}:*Ccnd3*^{-/-}:*Tcrb* thymuses also contain primarily DP cells, but at dramatically reduced numbers (1.5×10^7 cells). When probing endogenous *Tcrb* loci, RAG1^{-/-}:*Ccnd3*^{-/-}:*Tcrb* DP thymocytes exhibit no defects in short-range interactions between Eβ and the Dβ1 region compared with their proliferation-competent RAG1^{-/-}:*Tcrb* DP counterparts (Fig. 4B). Importantly, preferential dissociation of the distal *Trbv* domain is unaffected in *Ccnd3*^{-/-} DP thymocytes when these interactions are measured from two independent viewpoints within the RC (Fig. 4C, 4D).

We also examined global conformational changes at *Tcrb* in RAG1^{-/-}:*Ccnd3*^{-/-}:*Tcrb* thymocytes using 3D-FISH. We first sorted DN and DP cells from these animals to remove contaminating CD8⁺ cells (Fig. 4A), which represent an intermediate between the DN and DP stages (49). Fixed cells were hybridized to fluorescent probes for regions at the very 5' end of *Tcrb* and near the RC (Fig. 4B, top), with probe separation used as a metric for locus contraction. As shown in Fig. 4E, *Tcrb* is contracted in RAG1^{-/-}:*Ccnd3*^{-/-}:*Tcrb* DN thymocytes compared with DP cells. In fact, locus decontraction is statistically indistinguishable in DP thymocytes derived from *Ccnd3*-deficient and -sufficient animals. Taken together, the low- (FISH) and high-resolution (3C) data indicate that dissociation of the distal *Trbv* and RC domains is independent of the massive proliferative burst that precedes DP thymocyte differentiation and, instead, may be mediated by DP-intrinsic mechanisms.

The hinge region for dissociation of distal *Trbvs* is unaltered epigenetically and transcriptionally during thymocyte development

To gain a better understanding of mechanisms that control specific dissociation of the distal *Trbv* domain in DP thymocytes, we used 3C to map the inflection point between retained and lost RC interactions. Our initial 3C analyses (Fig. 1C) suggested that the transition occurred in a 40-kb window upstream of *Trbv12-1* (retained RC interaction) and *Trbv5* (lost RC interaction). A more refined 3C “walk,” using Eβ as the viewpoint, revealed a transition between two adjacent restriction fragments, which have similar (*Trbv11*) or substantially diminished (5'V11) interaction with Eβ when comparing DN to DP thymocytes (Fig. 5A, left). All additional restriction fragments tested upstream of 5'V11, including those spanning distal *Trbv* segments, exhibit diminished association with Eβ in DP relative to DN cells (Figs. 1A, 1C, 5A). The topological transition in DP thymocytes is also evident when two independent viewpoints are used near the RC (Dβ2 and 5'PC, Fig. 5B, right). Importantly, complementary 3C experiments, using viewpoints at this topological transition within the *Trbv* cluster,

FIGURE 3. Architectural proteins and chromatin boundaries are retained in DN and DP thymocytes. **(A) Top.** Published ChIP-seq profile for CTCF binding in RAG-deficient DN thymocytes (36). ChIP-qPCR data for CTCF and RAD21 occupancy (*middle and bottom*, respectively) are shown for DN versus DP thymocytes. Background levels of signal were determined using total IgG as a ChIP Ab (black bar). Data are presented as means \pm SEM of percentage input signal from three independent experiments. Statistically significant differences between DN and DP samples are represented as $*p < 0.05$ (Student *t* test). **(B)** *Prss2* expression was quantified relative to *Actb* using RT-qPCR assays in the indicated cell types (22). Mean values from three independent experiments are shown (\pm SEM). **(C) Top.** Schematic of the barrier region upstream of *Tcrb*-RC is shown with red nucleosomes denoting repressive chromatin and green nucleosomes representing active chromatin. Locations of qPCR primers used for H3K4me2 ChIP are shown under the cartoon. *Bottom.* ChIP-qPCR data for H3K4me2, presented as percentage input chromatin (\pm SEM) from three independent experiments. Statistically significant differences between Δ PD β 1 and DP samples are represented as $*p < 0.05$ (Student *t* test).



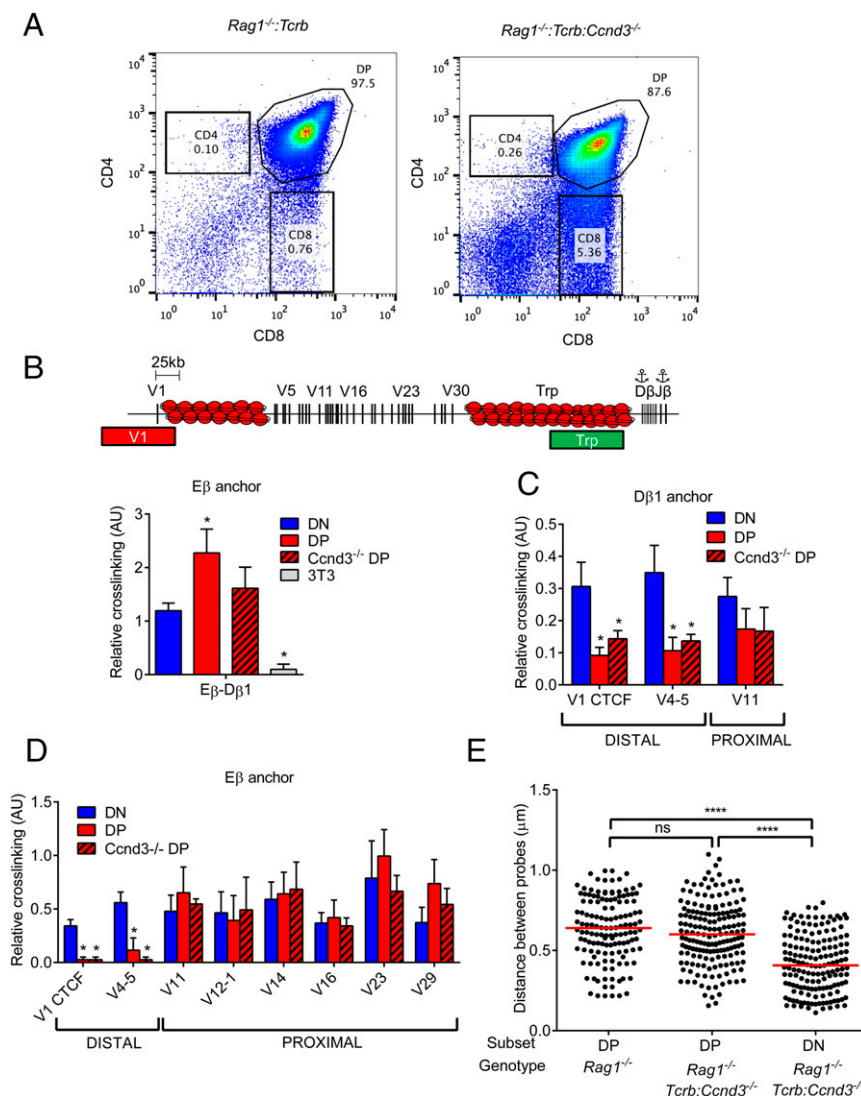
supported our conclusions. Association between a restriction fragment spanning *Trbv11* and a fragment within the RC is indistinguishable in DN and DP thymocytes (Fig. 5C, *right*), whereas 3C data from the 5'V11 viewpoint reflects its dissociation from the RC during this developmental transition (Fig. 5C, *left*). Therefore, the region located directly upstream of *Trbv11* serves as a “hinge” for developmentally regulated dissociation of distal V β gene segments from the RC in DP thymocytes.

We next explored potential mechanisms controlling this developmental hinge, focusing on specific changes to chromatin that may occur in this region during the DN to DP transition. First, binding of CTCF and RAD21 to a site nearest the hinge region is unaltered in DP compared with DN thymocytes (Fig. 5D). Second, transcription of two long interspersed element repetitive elements located 3' of *Trbv11* is repressed in DP thymocytes, which is similar to reduced expression of all germline *Trbv* segments in these cells (Fig. 5E). Third, similar to transcription, histone acetylation at sites within the hinge region also diminishes during transition to the DP subset (Fig. 5F). Thus, the hinge region exhibits no obvious epigenetic or transcriptional characteristics distinguishing it from developmental changes that occur over the entire *Trbv* cluster.

Stage-specific dissociation of distal *Trbv* segments on functionally rearranged alleles

Our data suggest that, on germline *Tcrb* alleles in RAG-deficient mice, the distal *Trbv* domain separates spatially from the RC in DP thymocytes via mechanisms independent of 5'PC function. During normal T cell development, the DN to DP transition is driven by functional *Tcrb* rearrangements, which are usually restricted to a single allele in each cell (6). All long-range recombination events between upstream V β segments and the RC will delete 5'PC. Moreover, a large subset of these rearrangements also deletes the inflection point for dissociation of distal V β segments from the RC, positioned upstream of *Trbv11*. Thus, examination of *Tcrb* conformation on a more physiologic allele, harboring a distal *Trbv* rearrangement, would provide an independent test for whether 5'PC or the 5'V11 hinge region is involved in stage-specific separation of distal *Trbv* segments.

For this purpose, we performed 3C analyses on thymocytes from a mouse strain that harbors two functional V β 5D β 1J β 1.4 alleles in their germline (Fig. 6A), termed V β 1NT mice (38). Whereas the remaining *Trbvs* on this allele can rearrange to D β 2J β 2 segments in DN thymocytes, recombination of these upstream V β segments is repressed in DP cells (39). In the RAG1^{-/-} genetic background,

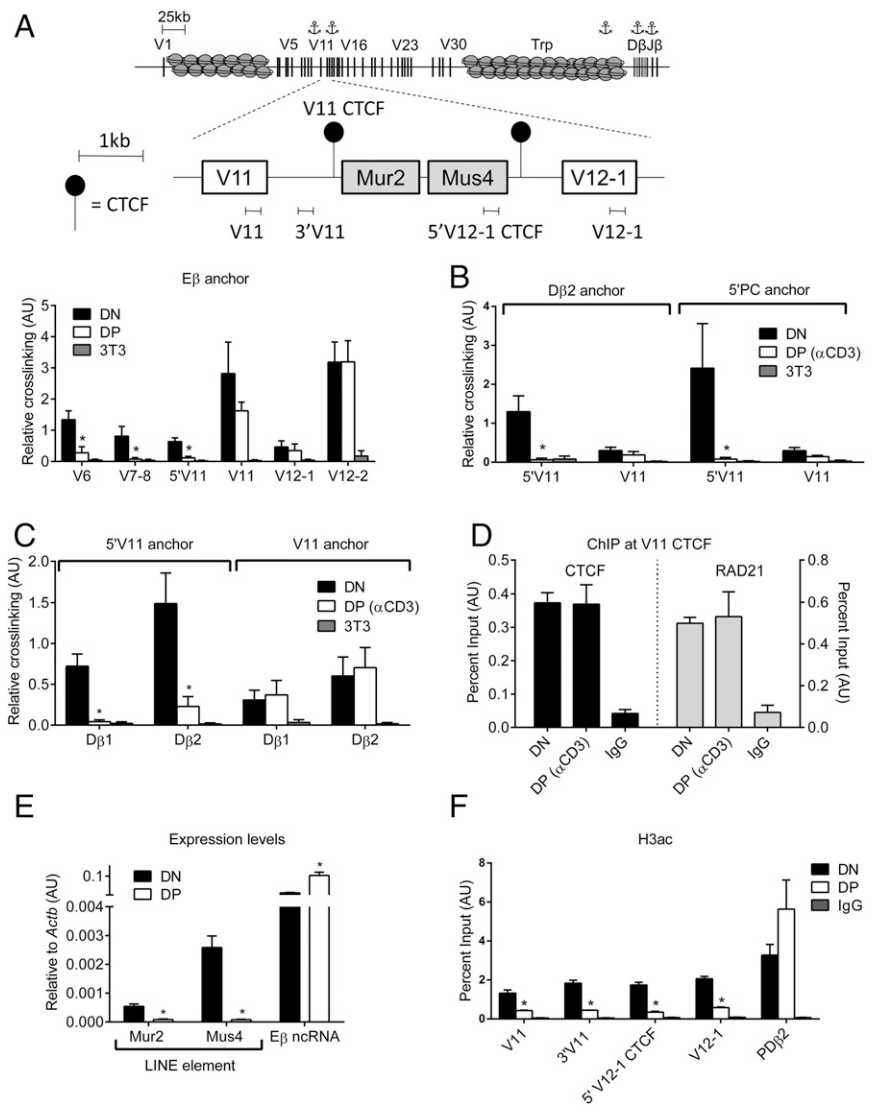


the V β 1NT allele drives developmental progression of thymocytes to the DP stage (39). Thus, to assess *Tcrb* conformation in DN thymocytes, pre-TCR signaling was crippled in RAG1^{-/-}:V β 1NT mice by making them homozygous for a null mutation in the LAT adaptor molecule (38, 39). As shown in Fig. 6A, the E β enhancer associates not only with the rearranged V β 5D β 1J β 1.4 exon in DN cells, but also with the remaining unrearranged *Trbv* segments, including *Trbv1* situated ~150 kb upstream. Enhancer interactions with the *Trbv* segments are cell type specific because they are diminished significantly in pro-B cells from the RAG1^{-/-}:LAT^{-/-}:V β 1NT mice (Fig. 6A). In DP thymocytes from RAG1^{-/-}:V β 1NT mice, short-range interactions between E β and D β 2 are retained (Fig. 6A, right), as well as those with the rearranged *Trbv4/5* region (Fig. 6A, left). However, the enhancer no longer associates with more distal *Trbv1*–3 gene segments. Dissociation is not solely due to enhancer capture by the promoter of the rearranged *Trbv5*, because we find a parallel loss of interactions between the distal *Trbv1* segment and a second viewpoint within the RC spanning the D β 2J β cluster (Fig. 6B).

To determine whether intra-V β interactions are maintained on the rearranged allele following differentiation to the DP subset, we performed 3C analyses using *Trbv2* as the viewpoint. As shown in Fig. 6C, association between *Trbv2* and *Trbv1* on the rearranged V β 1NT allele, observed in DN thymocytes, is largely lost upon transition to the DP stage. In contrast, *Trbv1*–2 association is

maintained on DP thymocytes with germline *Tcrb* alleles, further confirming that the folded configuration of the distal *Trbv* domain is retained in these cells (Fig. 2B). As expected, *Trbv2* dissociates from the RC in DP thymocytes harboring either the rearranged or germline allele. Thus, although RC-distal V β interactions are disrupted on both types of alleles, the conformational impact of DP differentiation on the distal V β cluster appears to be distinct for *Tcrb* loci with a germline (remains folded) versus the V β 1NT configuration (unravels). Underlying mechanisms for this distinction remain to be determined; however, multiple CTCF sites are deleted from the rearranged V β 1NT allele, which may preclude intra-V β folding, once these segments dissociate from the RC. Future studies could address this issue by examining new *Tcrb* alleles that have rearranged to more RC-proximal V β segments, and thus retain a fuller complement of CTCF sites.

Diminished RC–*Trbv* looping upstream of the preassembled V β D β J β exon in DP thymocytes does not correlate with reduced deposition of CTCF at any site along the V β 1NT allele (Fig. 6D). Similarly, RAD21 levels are not significantly altered at any of these CTCF sites, with the exception of a site situated 5' to the rearranged *Trbv5* segment, where RAD21 binding is reduced (Fig. 6E). However, the functional significance of reduced cohesin deposition at this single site remains unclear. Notwithstanding, we show that spatial segregation of distal *Trbv* segments from the RC in DP thymocytes is a common feature of germline, as well as



rearranged, *Tcrb* alleles (Fig. 7). Dissociation of the distal *Trbv* domain in DP thymocytes occurs regardless of whether the 5'PC tether or the 5'V11 inflection regions are present. These data strongly suggest that separation of distal Vβ segments is independent of specific *cis*-acting elements and is a process inherent to thymocytes transitioning from the DN to DP stage.

Discussion

The assembly of large AgR loci during lymphocyte development is controlled by coordinated changes in transcription, chromatin, and conformation (1–5). At the appropriate developmental stage for assembly, recombinase targets within each AgR locus become transcriptionally active and long-range recombination is facilitated by locus contraction (10). For *Igh* and *Tcrb*, these features are reversed at subsequent stages of development to enforce allelic exclusion, despite continued expression of the V(D)J recombinase (17, 20, 45, 46). With regard to locus conformation, it has been thought that *Igh* and *Tcrb* decontraction is accompanied by the loss of spatial associations between their respective RCs and V clusters (20, 32). In this work, we provide the most rigorous examination to date of this model, using high-resolution 3C to probe spatial associations within *Tcrb* as thymocytes pass from the permissive DN stage of development to the DP subset, in which its allelic exclusion is enforced.

A major finding from our 3C studies is that most of the *Trbv* cluster remains associated with the RC after transition of thymocytes to the DP stage and after *Tcrb* locus decontraction (Fig. 7). Only the most distal portion of the *Trbv* cluster, upstream from the *Trbv11* gene segment, spatially segregates from the RC. These conformational and cell imaging data remain consistent with one another, because all previous 3D-FISH assays, including our own, employed probes for the most distal *Trbv* domain, which separates to a greater average distance from RC probes in DP thymocytes (20, 22). Although only distal Vβ segments dissociate from the RC, both the proximal and distal *Trbv* domains appear to remain folded in their thymocyte-specific conformations, which promotes domain-specific association of gene segments (Fig. 7). Of note, our conclusions differ significantly from those of a published study that also used 3C to probe *Tcrb* conformations in DN and DP thymocytes (20). The authors of the previous study concluded that both *Trbv*–RC and *Trbv*–*Trbv* interactions are disrupted in DP cells over the entire Vβ cluster. The specific source of this discrepancy remains unclear; however, the previous study used DN thymocytes cultured on stromal cells and older methods for 3C analyses that are, at best, only semiquantitative.

Notwithstanding, our data clearly preclude a model in which *Tcrb* allelic exclusion is enforced primarily by topological dissociation of the *Trbv* cluster from its DβJβ targets in DP thy-

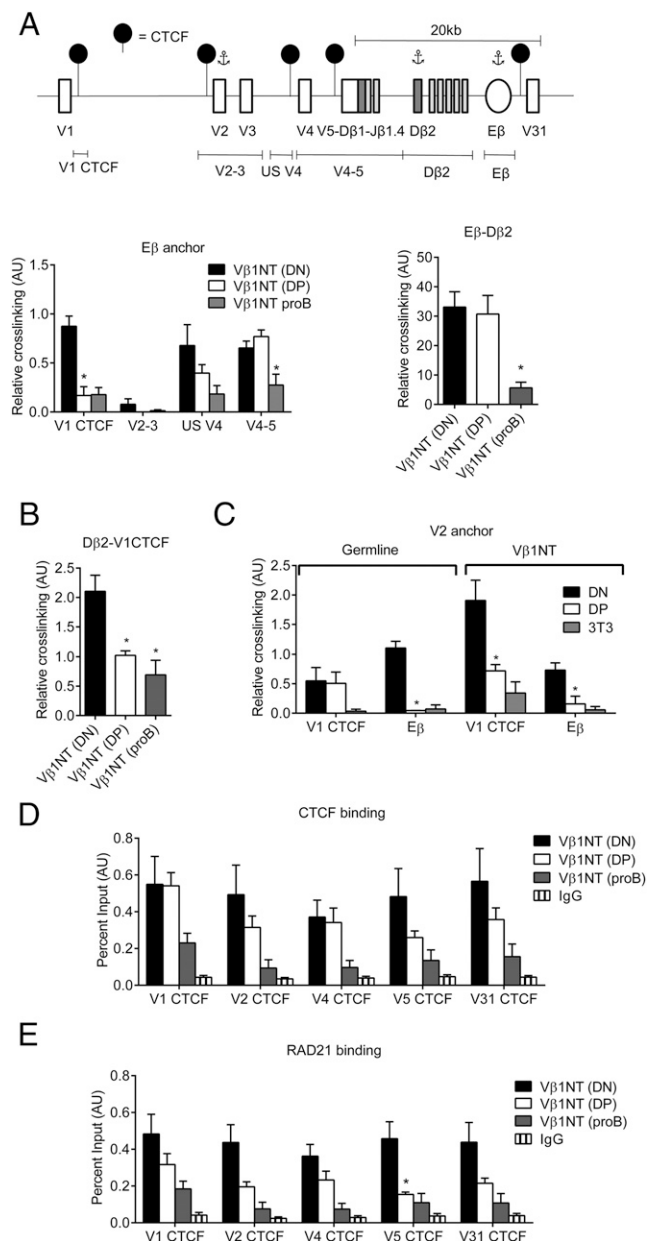


FIGURE 6. DP-specific dissociation of distal *Trbv* segments on a rearranged *Tcrb* allele. **(A)** Schematic of the rearranged *Tcrb* locus in Vβ1NT mice. Location of CTCF binding sites within the region are designated as black lollipops. HindIII fragments used for 3C-qPCR analysis are shown below the cartoon. 3C analysis was performed using the Eβ viewpoint (denoted by the anchor symbol), probing its interactions with either the upstream *Trbv* region (left) or with the nearby Dβ2Jβ cluster (right). Chromatin for these assays was obtained from purified pro-B cells or DP thymocytes harvested from RAG-deficient mice with the Vβ1NT rearrangement on both of their germline alleles. For corresponding DN thymocytes, the Vβ1NT allele was introduced into a RAG1^{-/-}:LAT^{-/-} background. **(B)** 3C-qPCR assays that measure interactions between the Dβ2 viewpoint and the most distal *Trbv1* region (respectively denoted by the anchor symbol). **(C)** 3C-qPCR assays measuring interactions between the distal *Trbv2* viewpoint and either the V1-CTCF or Eβ regions in germline (left) versus rearranged *Tcrb* alleles (Vβ1NT, right). **(D)** and **(E)** ChIP-qPCR assays were performed to quantify CTCF (C) and RAD21 deposition (D) at the indicated sites. Statistically significant differences are denoted as **p* < 0.05 (Student *t* test).

mocytes. Although this spatial mechanism may be dominant for *Trbv1*–5, the only functional Vβ segments that separate from the RC, distinct factors must prevent long-range recombination of the

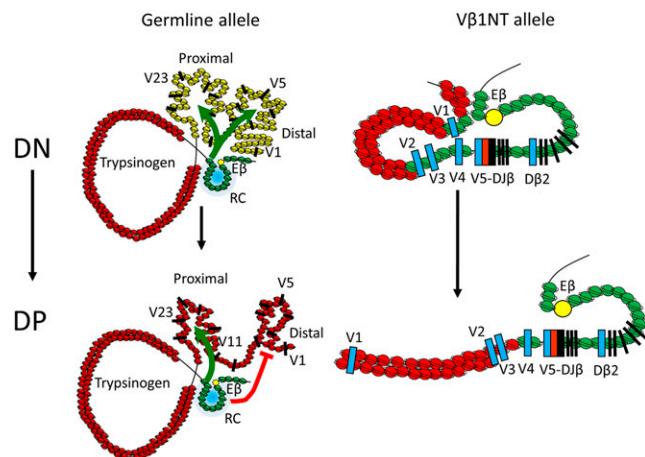


FIGURE 7. Model for developmental reconfiguration of *Tcrb*. Cartoon depictions of germline (left) and rearranged (right) *Tcrb* loci in either DN (top) or DP (bottom) thymocytes. Distinct types of chromatin and transcriptional activity are represented by colored nucleosomes: repressive, transcriptionally inert (red); highly transcribed, accessible (green); modestly transcribed, accessible (yellow). **Left:** Folding of the distal (containing V1 and V5) and proximal (containing V23) *Trbv* domains, as well as their interactions with the RC/Eβ region on a germline *Tcrb* allele, are highlighted as green arrows. In DP thymocytes with a germline *Tcrb*, both *Trbv* domains remain folded but only the distal domain dissociates from the RC (red block). **Right:** Similarly, distal *Trbv* segments that remain on a rearranged *Tcrb* allele (e.g., V1) spatially segregate from the Eβ interactome in DP thymocytes.

other 16 Vβ segments, which remain associated with the RC in DP thymocytes. Thus, for this latter set of Vβ segments, transcriptional suppression in DP cells is the most likely mechanism for enforcing allelic exclusion. In this regard, we have shown that, in DN thymocytes, the relative levels of spatial proximity for each *Trbv* segment do not contribute in a measurable way to their usage in the preselection *Tcrb* repertoire (7). Instead, the level of transcription for each *Trbv* segment provides an excellent correlate for its usage in Vβ-to-DβJβ recombination. We conclude that Vβ promoter activity, rather than spatial constraints, is a dominant mechanism for both *Tcrb* gene assembly in DN cells and its subsequent allelic exclusion in DP thymocytes.

We also assessed possible mechanisms that may drive *Tcrb* conformational changes during thymocyte development. Our analyses discount domain-specific changes in transcription or general chromatin features as a force for the preferential dissociation of distal *Trbv* segments from the RC. All of these features appear to be regulated coordinately over the entire *Trbv* cluster, including the mapped inflection point for RC dissociation near *Trbv11*. Moreover, loss of distal *Trbv*–RC interactions in DP cells is independent of CTCF/cohesin deposition at specific sites within the Vβ cluster or at their tether near the RC. We also found that *Tcrb* decontraction and distal *Trbv* dissociation from the RC are both independent of the massive proliferative burst preceding DN to DP transition.

The latter finding suggests that *Tcrb* conformational remodeling occurs via a DP-intrinsic process. Indeed, this model is strongly supported by our topological analyses of a functionally rearranged *Tcrb* allele. In DN thymocytes, upstream *Trbv* segments remain associated with an RC that harbors a functional Vβ5Dβ1Jβ1.4 rearrangement (Fig. 7). Similar to germline *Tcrb* loci, the distal *Trbv* segments become transcriptionally repressed (38, 39, 45) and dissociate from the RC interactome in DP thymocytes. The spatial segregation occurs on a rearranged allele that lacks both the normal long-range tether for distal Vβ segments (5'PC) and the

mapped inflection point for *Trbv*-RC associations in DP cells (5'V11). These findings indicate that, rather than specific *cis*-elements orchestrating *Tcrb* conformational changes, perhaps spatial segregation of distal *Trbv* segments occurs via a process that is intrinsic to DP thymocytes. In fact, a switch from RC association with entire V clusters at the earliest precursor stages to a loss of RC-distal V interactions at subsequent stages may be a general feature of lymphocyte development. In DN thymocytes, distal and proximal V segments associate with RCs at both *Tcrb* (this study) and *Tcrad* (33). In the latter case, a global V-RC interactome likely facilitates more diverse usage of V segments in assembled *Tcrd* genes. However, upon transition to the DP stage, distal portions of both the *Trbv* and *Trav* clusters dissociate from the RC, which limits initial *Tcrd* recombination to the most proximal V α segments (33). For *Tcrb*, DP-intrinsic dissociation of distal V β segments might curb their secondary rearrangement to the downstream D β 2J β cluster, if present, which would delete an existing V β D β 1J β join. Likewise, in pro-B cells, distal V segments at both the *Igh* and *Igk* loci associate with their RCs (34, 50); however, whether these long-range interactions are maintained in pre-B cells remains an open question.

In the case of thymocyte development, future studies must focus on mechanisms driving the stage-specific changes in *Tcrb* conformation. One attractive possibility for an underlying mechanism is stage-specific alteration of transcriptional status over the entire *Trbv* cluster. Our prior studies have shown that the *Trbv* domains fold and interact with distant D β J β cluster in DN thymocytes, independent of RC transcription (22). Because many V β segments become transcriptionally active upon their differentiation to the DN stage, we speculate that the induced expression dictates conformational changes that drive RC-V association upon T cell commitment. Likewise, dissociation of the distal *Trbv* domain is accompanied by a widespread loss of V β transcription (45, 46). Perhaps both of these expression-induced changes in conformation are governed by the activation or suppression of a key transcription factor, such as E2A, which has been implicated in the control of V β -to-D β J β recombination (51).

Even so, a critical question would be why only the most distal V β segments dissociate in DP cells, despite the loss of transcription over the entire *Trbv* cluster. We suspect that clues can be derived from our finding that 5'V11 serves as a hinge for the loss of RC interactions on germline *Tcrb* alleles in DP thymocytes. The *Trbv11* region is the transition from a large stretch of pseudogene segments, *Trbv6-11*, which are expressed at very low steady-state levels and lack active chromatin modifications (7, 44), to the most highly active cluster of *Trbv* segments (*Trbv12-13*) in DN thymocytes, the latter of which remain partially active in DP cells (see Fig. 1G). In this regard, genome-wide conformation studies have shown that regions of similar transcriptional status tend to form topologically associated domains (52). Thus, in DP thymocytes, silencing of the distal V β segments may drive their preferential association with neighboring regions of repressed transcription, including the silent trypsinogen genes between *Trbv1* and *Trbv2* and pseudogenes that encompass the 5' portion of the locus (Fig. 7). These changes would spatially segregate *Trbv1-11* from the modestly transcribed *Trbv12-13* and other downstream segments, which retain their association with the RC via thymocyte-intrinsic mechanisms. Future investigations of such conformational changes at AgR loci will continue to shed light on the mechanisms controlling genome topologies and how these changes, in turn, regulate many aspects of gene function.

Disclosures

The authors have no financial conflicts of interest.

References

- Bassing, C. H., W. Swat, and F. W. Alt. 2002. The mechanism and regulation of chromosomal V(D)J recombination. *Cell* 109(Suppl.): S45-S55.
- Osipovich, O., and E. M. Oltz. 2010. Regulation of antigen receptor gene assembly by genetic-epigenetic crosstalk. *Semin. Immunol.* 22: 313-322.
- Krangel, M. S. 2009. Mechanics of T cell receptor gene rearrangement. *Curr. Opin. Immunol.* 21: 133-139.
- Bossen, C., R. Mansson, and C. Murre. 2012. Chromatin topology and the regulation of antigen receptor assembly. *Annu. Rev. Immunol.* 30: 337-356.
- Roy, A. L., R. Sen, and R. G. Roeder. 2011. Enhancer-promoter communication and transcriptional regulation of *Igh*. *Trends Immunol.* 32: 532-539.
- Brady, B. L., N. C. Steinle, and C. H. Bassing. 2010. Antigen receptor allelic exclusion: an update and reappraisal. *J. Immunol.* 185: 3801-3808.
- Gopalakrishnan, S., K. Majumder, A. Predeus, Y. Huang, O. I. Koues, J. Verma-Gaur, S. Loguercio, A. I. Su, A. J. Feeney, M. N. Artyomov, and E. M. Oltz. 2013. Unifying model for molecular determinants of the preselection V β repertoire. *Proc. Natl. Acad. Sci. USA* 110: E3206-E3215.
- Choi, N. M., S. Loguercio, J. Verma-Gaur, S. C. Degner, A. Torkamani, A. I. Su, E. M. Oltz, M. Artyomov, and A. J. Feeney. 2013. Deep sequencing of the murine *Igh* repertoire reveals complex regulation of nonrandom V gene rearrangement frequencies. *J. Immunol.* 191: 2393-2402.
- Zhang, Y., R. P. McCord, Y. J. Ho, B. R. Lajoie, D. G. Hildebrand, A. C. Simon, M. S. Becker, F. W. Alt, and J. Dekker. 2012. Spatial organization of the mouse genome and its role in recurrent chromosomal translocations. *Cell* 148: 908-921.
- Cobb, R. M., K. J. Oestreich, O. A. Osipovich, and E. M. Oltz. 2006. Accessibility control of V(D)J recombination. *Adv. Immunol.* 91: 45-109.
- Matthews, A. G., A. J. Kuo, S. Ramon-Maiques, S. Han, K. S. Champagne, D. Ivanov, M. Gallardo, D. Carney, P. Cheung, D. N. Ciccone, et al. 2007. RAG2 PHD finger couples histone H3 lysine 4 trimethylation with V(D)J recombination. *Nature* 450: 1106-1110.
- Liu, Y., R. Subrahmanyam, T. Chakraborty, R. Sen, and S. Desiderio. 2007. A plant homeodomain in RAG-2 that binds hypermethylated lysine 4 of histone H3 is necessary for efficient antigen-receptor-gene rearrangement. *Immunity* 27: 561-571.
- Ji, Y., W. Resch, E. Corbett, A. Yamane, R. Casellas, and D. G. Schatz. 2010. The in vivo pattern of binding of RAG1 and RAG2 to antigen receptor loci. *Cell* 141: 419-431.
- Yang, Q., J. Jeremiah Bell, and A. Bhandoola. 2010. T-cell lineage determination. *Immunol. Rev.* 238: 12-22.
- Bouvier, G., F. Watrin, M. Naspetti, C. Verthuy, P. Naquet, and P. Ferrier. 1996. Deletion of the mouse T-cell receptor beta gene enhancer blocks $\alpha\beta$ T-cell development. *Proc. Natl. Acad. Sci. USA* 93: 7877-7881.
- Oestreich, K. J., R. M. Cobb, S. Pierce, J. Chen, P. Ferrier, and E. M. Oltz. 2006. Regulation of TCR β gene assembly by a promoter/enhancer holocomplex. *Immunity* 24: 381-391.
- Kosak, S. T., J. A. Skok, K. L. Medina, R. Riblet, M. M. Le Beau, A. G. Fisher, and H. Singh. 2002. Subnuclear compartmentalization of immunoglobulin loci during lymphocyte development. *Science* 296: 158-162.
- Hewitt, S. L., J. Chaumeil, and J. A. Skok. 2010. Chromosome dynamics and the regulation of V(D)J recombination. *Immunol. Rev.* 237: 43-54.
- Shih, H. Y., and M. S. Krangel. 2013. Chromatin architecture, CCCTC-binding factor, and V(D)J recombination: managing long-distance relationships at antigen receptor loci. *J. Immunol.* 190: 4915-4921.
- Skok, J. A., R. Gisler, M. Novatchkova, D. Farmer, W. de Laat, and M. Busslinger. 2007. Reversible contraction by looping of the *Tcrd* and *Tcrb* loci in rearranging thymocytes. *Nat. Immunol.* 8: 378-387.
- Schlimgen, R. J., K. L. Reddy, H. Singh, and M. S. Krangel. 2008. Initiation of allelic exclusion by stochastic interaction of *Tcrb* alleles with repressive nuclear compartments. *Nat. Immunol.* 9: 802-809.
- Majumder, K., O. I. Koues, E. A. Chan, K. E. Kyle, J. E. Horowitz, K. Yang-Iott, C. H. Bassing, I. Taniuchi, M. S. Krangel, and E. M. Oltz. 2015. Lineage-specific compaction of *Tcrb* requires a chromatin barrier to protect the function of a long-range tethering element. *J. Exp. Med.* 212: 107-120.
- Phillips, J. E., and V. G. Corces. 2009. CTCF: master weaver of the genome. *Cell* 137: 1194-1211.
- Kim, T. H., Z. K. Abdullaev, A. D. Smith, K. A. Ching, D. I. Loukinov, R. D. Green, M. Q. Zhang, V. V. Lobanenko, and B. Ren. 2007. Analysis of the vertebrate insulator protein CTCF-binding sites in the human genome. *Cell* 128: 1231-1245.
- Parelho, V., S. Hadjur, M. Spivakov, M. Leleu, S. Sauer, H. C. Gregson, A. Jarmuz, C. Canzonetta, Z. Webster, T. Nesterova, et al. 2008. Cohesins functionally associate with CTCF on mammalian chromosome arms. *Cell* 132: 422-433.
- Guo, C., H. S. Yoon, A. Franklin, S. Jain, A. Ebert, H. L. Cheng, E. Hansen, O. Despo, C. Bossen, C. Vettermann, et al. 2011. CTCF-binding elements mediate control of V(D)J recombination. *Nature* 477: 424-430.
- Lin, S. G., C. Guo, A. Su, Y. Zhang, and F. W. Alt. 2015. CTCF-binding elements 1 and 2 in the *Igh* intergenic control region cooperatively regulate V(D)J recombination. *Proc. Natl. Acad. Sci. USA* 112: 1815-1820.
- Degner, S. C., J. Verma-Gaur, T. P. Wong, C. Bossen, G. M. Iverson, A. Torkamani, C. Vettermann, Y. C. Lin, Z. Ju, D. Schulz, et al. 2011. CCCTC-binding factor (CTCF) and cohesin influence the genomic architecture of the *Igh* locus and antisense transcription in pro-B cells. *Proc. Natl. Acad. Sci. USA* 108: 9566-9571.
- Xiang, Y., S. K. Park, and W. T. Garrard. 2013. V κ gene repertoire and locus contraction are specified by critical DNase I hypersensitive sites within the V κ -J κ intervening region. *J. Immunol.* 190: 1819-1826.

30. Seitan, V. C., B. Hao, K. Tachibana-Konwalski, T. Lavagnoli, H. Mira-Bontenbal, K. E. Brown, G. Teng, T. Carroll, A. Terry, K. Horan, et al. 2011. A role for cohesin in T-cell-receptor rearrangement and thymocyte differentiation. *Nature* 476: 467–471.
31. Sicinska, E., I. Aifantis, L. Le Cam, W. Swat, C. Borowski, Q. Yu, A. A. Ferrando, S. D. Levin, Y. Geng, H. von Boehmer, and P. Sicinski. 2003. Requirement for cyclin D3 in lymphocyte development and T cell leukemias. *Cancer Cell* 4: 451–461.
32. Roldán, E., M. Fuxa, W. Chong, D. Martinez, M. Novatchkova, M. Busslinger, and J. A. Skok. 2005. Locus “decontraction” and centromeric recruitment contribute to allelic exclusion of the immunoglobulin heavy-chain gene. *Nat. Immunol.* 6: 31–41.
33. Shih, H. Y., and M. S. Krangel. 2010. Distinct contracted conformations of the *Tcrα/Tcrδ* locus during *Tcrα* and *Tcrδ* recombination. *J. Exp. Med.* 207: 1835–1841.
34. Stadhouders, R., M. J. de Bruijn, M. B. Rother, S. Yuvaraj, C. Ribeiro de Almeida, P. Kolovos, M. C. Van Zelm, W. van Ijcken, F. Grosveld, E. Soler, and R. W. Hendriks. 2014. Pre-B cell receptor signaling induces immunoglobulin κ locus accessibility by functional redistribution of enhancer-mediated chromatin interactions. *PLoS Biol.* 12: e1001791.
35. Shinkai, Y., and F. W. Alt. 1994. CD3ε-mediated signals rescue the development of CD4⁺CD8⁺ thymocytes in RAG-2^{-/-} mice in the absence of TCR β chain expression. *Int. Immunol.* 6: 995–1001.
36. Shih, H. Y., J. Verma-Gaur, A. Torkamani, A. J. Feeney, N. Galjart, and M. S. Krangel. 2012. *Tcrα* gene recombination is supported by a *Tcrα* enhancer- and CTCF-dependent chromatin hub. *Proc. Natl. Acad. Sci. USA* 109: E3493–E3502.
37. Shinkai, Y., S. Koyasu, K. Nakayama, K. M. Murphy, D. Y. Loh, E. L. Reinherz, and F. W. Alt. 1993. Restoration of T cell development in RAG-2-deficient mice by functional TCR transgenes. *Science* 259: 822–825.
38. Brady, B. L., M. A. Oropallo, K. S. Yang-Iott, T. Serwold, K. Hochedlinger, R. Jaenisch, I. L. Weissman, and C. H. Bassing. 2010. Position-dependent silencing of germline Vβ segments on TCRβ alleles containing preassembled VβDJβCP1 genes. *J. Immunol.* 185: 3564–3573.
39. Brady, B. L., and C. H. Bassing. 2011. Differential regulation of proximal and distal Vβ segments upstream of a functional VDJβ1 rearrangement upon β-selection. *J. Immunol.* 187: 3277–3285.
40. Medvedovic, J., A. Ebert, H. Tagoh, I. M. Tamir, T. A. Schwickert, M. Novatchkova, Q. Sun, P. J. Huis In 't Veld, C. Guo, H. S. Yoon, et al. 2013. Flexible long-range loops in the V_H gene region of the *Igh* locus facilitate the generation of a diverse antibody repertoire. *Immunity* 39: 229–244.
41. Langmead, B., and S. L. Salzberg. 2012. Fast gapped-read alignment with Bowtie 2. *Nat. Methods* 9: 357–359.
42. Thongjuea, S., R. Stadhouders, F. G. Grosveld, E. Soler, and B. Lenhard. 2013. r3Cseq: an R/Bioconductor package for the discovery of long-range genomic interactions from chromosome conformation capture and next-generation sequencing data. *Nucleic Acids Res.* 41: e132–e132.
43. Rice, P., I. Longden, and A. Bleasby. 2000. EMBOSS: the European molecular biology open software suite. *Trends Genet.* 16: 276–277.
44. Pekowska, A., T. Benoukraf, J. Zacarias-Cabeza, M. Belhocine, F. Koch, H. Holota, J. Imbert, J. C. Andrau, P. Ferrier, and S. Spicuglia. 2011. H3K4 trimethylation provides an epigenetic signature of active enhancers. *EMBO J.* 30: 4198–4210.
45. Senoo, M., and Y. Shinkai. 1998. Regulation of Vβ germline transcription in RAG-deficient mice by the CD3ε-mediated signals: implication of Vβ transcriptional regulation in TCRβ allelic exclusion. *Int. Immunol.* 10: 553–560.
46. Tripathi, R., A. Jackson, and M. S. Krangel. 2002. A change in the structure of Vβ chromatin associated with TCR β allelic exclusion. *J. Immunol.* 168: 2316–2324.
47. Chattopadhyay, S., C. E. Whitehurst, F. Schwenk, and J. Chen. 1998. Biochemical and functional analyses of chromatin changes at the TCR-β gene locus during CD4⁺CD8⁺ to CD4⁺CD8⁺ thymocyte differentiation. *J. Immunol.* 160: 1256–1267.
48. Naumova, N., M. Imakaev, G. Fudenberg, Y. Zhan, B. R. Lajoie, L. A. Mirny, and J. Dekker. 2013. Organization of the mitotic chromosome. *Science* 342: 948–953.
49. Serwold, T., K. Hochedlinger, M. A. Inlay, R. Jaenisch, and I. L. Weissman. 2007. Early TCR expression and aberrant T cell development in mice with endogenous prereduced T cell receptor genes. *J. Immunol.* 179: 928–938.
50. Lin, Y. C., C. Benner, R. Mansson, S. Heinz, K. Miyazaki, M. Miyazaki, V. Chandra, C. Bossen, C. K. Glass, and C. Murre. 2012. Global changes in the nuclear positioning of genes and intra- and interdomain genomic interactions that orchestrate B cell fate. *Nat. Immunol.* 13: 1196–1204.
51. Agata, Y., N. Tamaki, S. Sakamoto, T. Ikawa, K. Masuda, H. Kawamoto, and C. Murre. 2007. Regulation of T cell receptor β gene rearrangements and allelic exclusion by the helix-loop-helix protein, E47. *Immunity* 27: 871–884.
52. Dixon, J. R., S. Selvaraj, F. Yue, A. Kim, Y. Li, Y. Shen, M. Hu, J. S. Liu, and B. Ren. 2012. Topological domains in mammalian genomes identified by analysis of chromatin interactions. *Nature* 485: 376–380.